Characterization of GaAs and GaAs/Cr/GaAs interfacial layers fabricated via magnetron sputtering on silicon (100)

Camilo Pulzara-Mora[a], José Doria-Andrade[b], Roberto Bernal-Correa[c], Andrés Rosales-Rivera[d], Álvaro Pulzara-Mora[*a]

[a]*Laboratorio de Nanoestructuras Semiconductoras, Facultad de Ciencias Exactas y Naturales, Universidad Nacional de Colombia, Sede Manizales, Manizales 170004, Colombia.*

.[b]*Laboratorio de Materialografía, Facultad de Ingeniería, Institución Universitaria Pascual Bravo, Medellín, Colombia*

[c]*Instituto de Estudios de la Orinoquía, Universidad Nacional de Colombia, Sede Orinoquia, Kilometro 9 vía Arauca-Caño Limón, Arauca, Colombia*

[d] *Laboratorio de Magnetismo y Materiales Avanzados, Facultad de Ciencias Exactas y Naturales, Universidad Nacional de Colombia, Sede Manizales, Manizales 170004, Colombia.*

The obtaining and study of semiconductor materials have been topics of interest for decades. However, alternatives that allow greater versatility at the time of their application have yet to be explored, such as the inclusion of some transition metals. In this work, we report the obtaining of GaAs and GaAs/Cr/GaAs layers, which were prepared by r.f. magnetron sputtering on a Si (100) substrate by varying the deposition time of the intermediate Cr layer for t = 5 min and 10 min, respectively. Scanning electron microscopy in cross-section was carried out to determine the growth mode of the GaAs and GaAs/Cr/GaAs films. The percentage of the elements in the GaAs/Cr/GaAs thin films was determined through energy dispersive spectroscopy (EDS) in cross-sections along the entire layer thickness. X-ray diffraction and micro-Raman spectroscopy at room temperature were measured to analyze the formation of CrAs and GaCr binary phases by diffusion across interlayers. Finally, we conclude on the possible use of this technique to obtain semiconductor alloys with Cr inclusion.

(Received January 22, 2024; Accepted April 26, 2024)

Keywords: Magnetron sputtering, Raman spectroscopy, X-ray

1. Introduction

The increase in the use of III-V semiconductor materials in the optoelectronic industry poses a significant challenge for the scientific community in recent years [1,2]. It is necessary to reduce production costs, improve efficiency, and discover device designs that allow greater versatility in their applications. An example of the studies currently being carried out involves the doping of this type of semiconductor with transition metals such as Cr, Fe, Mn, among others. This coupling allows the combination of physical properties and, consequently, opens various fields of applicability [3,4]. In the case of GaAs (gallium arsenide), there already exists a substantial scientific and experimental knowledge base [5], making it a potential candidate for coupling with some of the mentioned elements [6,7].

Gallium arsenide is a semiconductor compound with a direct bandgap energy of 1.42 eV at room temperature, widely used in current technology due to its various applications as an infrared light emitter, high-efficiency solar cells ($\eta \sim 29\%$) [8], field-effect transistors [9], and ionizing radiation detection operating at room temperature [10]. Chromium is a transition metal of interest for developing room temperature ferromagnetism in III-V semiconductors such as GaN and GaAs [11-13]. In this case, the Cr atoms can substitute the gallium atoms in the metallic sublattice or be

* Corresponding author: aopulzaram@unal.edu.co
https://doi.org/10.15251/DJNB.2024.192.669

in the interstitial sites of the lattice. The doped Cr-GaAs compounds grown on GaAs semiconductor present a zinc-blende structure, with a half-metallic band structure. Cr-GaAs exhibits interesting ferromagnetic properties at room temperature because of the high Curie temperature (TC) predicted from ab initio theoretical calculations [14, 15]. It has been reported that for low-temperature anneals (Ta < 500 °C), Ga and As do not react with Cr at the interface. The interfacial reactions begin with the diffusion of the Cr transition metal into the GaAs at Ta > 500 °C, resulting in the formation of a possible compound Cr2X (X=Ga or As or both) [9]. Several properties of semi-insulating Cr-doped GaAs epitaxial layers grown by epitaxy techniques such as molecular beam epitaxy (MBE) [16], liquid-phase epitaxy (LPE) [17], and organometallic chemical vapor deposition (MOCVD) have been reported. However, the preparation of Cr-doped GaAs layers by non-epitaxial techniques, such as r.f. magnetron sputtering, has not been reported. Magnetron sputtering (MS) is a low-cost technique used in the semiconductor industry to grow thin films on isolated semiconductors and metal substrates for different applications [18,19]

In this study, we present the polycrystalline growth of GaAs and GaAs/Cr/GaAs layers by varying the deposition time of the Cr interlayer for tg = 5 min and 10 min. The aim is to investigate the diffusion of Cr across an interface and assess the formation of a secondary phase. Scanning electron microscopy (SEM) in cross-section was employed to determine the growth mode. Elemental chemical analysis using energy dispersive spectroscopy (EDS) along the entire thickness was conducted to analyze the formation of CrAs and CrGa secondary phases, indicative of the potential inclusion of Cr into the GaAs lattice. The crystal structure was further examined through X-ray diffraction (XRD) and Raman spectroscopy using backscattering geometry.

2. Experimental

2.1. Experimental conditions

The samples investigated in this study consist of a GaAs layer and GaAs bilayers with a Cr interlayer (GaAs/Cr/GaAs), where the deposition time of the Cr interlayer was varied. All samples were deposited using r.f. magnetron sputtering on (001) Si substrate in an Argon (Ar) atmosphere at a pressure of $5x10^{-3}$ Torr. Prior to each deposition run, the chamber's background pressure was maintained at $1x10^{-6}$ Torr. The Si (100) substrates underwent degreasing in acetone in an ultrasound bath for 10 minutes. The sample preparation process is detailed as follows: The GaAs layer was deposited for one hour at a substrate temperature of 580 °C, utilizing an r.f. power supply of 30 Watts on (100) Si substrate. For the GaAs/Cr/GaAs layers, a GaAs layer was first deposited on a Si substrate for 20 minutes at a substrate temperature of 500 °C. Subsequently, the substrate temperature was gradually decreased to 100 °C, over about 30 minutes to deposit a layer of Cr for 5 minutes (sample M1) and 10 minutes (sample M2). Finally, the substrate temperature was raised back to 500 °C, over about 30 minutes to deposit the second layer of GaAs for 20 minutes. R.F. power supplies for the GaAs and Cr targets were maintained at constant values of 30 and 10 Watts, respectively. After the deposition of the layers, the RF power and gas supply were turned off, and the samples were allowed to cool down to room temperature for approximately 6 hours. The experimental conditions are summarized in Table 1.

Table 1. Experimental growth conditions for the a GaAs layer and aAs/Cr/GaAs/Si(100) layers.

Parameter	Value
Background Pressure (Torr)	1.0×10^{-6}
Sputtering pressure (Torr)	5.0×10^{-3}
Target – substrate distance (cm)	5
Growth temperature of the GaAs layer (°C)	580
Growth temperature of GaAs/Cr/GaAs layers(°C)	500/100/500
Time growth of Cr on GaAs layer	5min and 10min

2.2. Characterization techniques

The thickness and composition of the layers were determined from SEM micrographs taken in cross-sections along the entire layer thickness deposited on a Si (100) substrate (scanning electron microscope FE-SEM on a JEOL JSM740 1F equipment). Crystal quality was assessed through X-ray diffraction (XRD) in the range of $2 < 2\theta < 120°$ using a Cu $K\alpha$ = 1.5405 Å as radiation source. Raman microscopy, configured in a backscattered mode with the direction perpendicular to the sample and an unpolarized beam, was employed to study the behavior of TO and LO vibrational modes of the GaAs and GaAs/Cr/GaAs layers. This was conducted using a Raman Dilor XY Labram spectrometer equipped with an Olympus BX40, utilizing a laser line of 632 nm with a power of 20 mW.

3. Results

3.1. Gallium arsenide (GaAs)

The results obtained from X-ray diffraction revealed that the GaAs layer deposited on (100) Si exhibited a zinc-blende (ZB)-type crystalline structure with a preferential orientation along the (111) direction, as illustrated in Fig. 1. The intensity of the peaks is sharp and narrow, indicating that the GaAs sample possesses good crystalline quality and a fine grain size. The (002) plane, located at $2\theta = 32.5°$, corresponds to the single crystal Si substrate used as a reference (Fig. 1). No additional diffraction peaks corresponding to GaAs phases were observed, providing evidence that the GaAs sample is crystalline. To avoid interference from the (004) main reflection plane of the Si (001) substrate located at $2\theta = 65°$, the spectrum is truncated at $2\theta = 60°$. The crystalline size, calculated using Scherrer's equation from the (111) plane, yielded a value of 28 nm, as shown in the inset of Fig. 1.

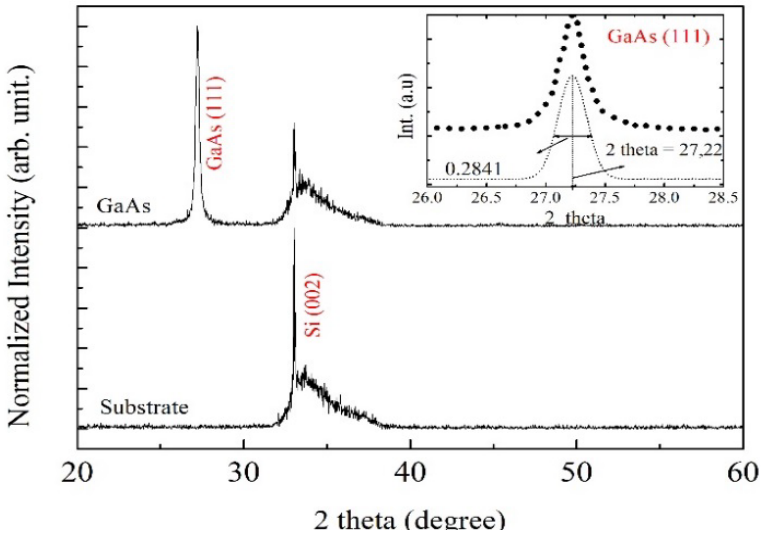

Fig. 1. a) X-ray spectra of a Si substrate used as a reference. b) X-ray spectra of a GaAs layer on (100) Si. The thicker line in the inset represents the deconvolution of the (111) GaAs plane into a Gaussian function achieved through curve fitting.

The morphological evaluation of the GaAs layer was also conducted using scanning electron microscopy, as depicted in Fig. 2. The figure presents cross-sectional SEM images captured along the entire layer thickness deposited on a Si (100) substrate, magnified at 50,000X with a scale of 100 nm. A distinct interface is evident between the layer and substrate. The images

reveal a typical columnar growth mode throughout the layer thickness, and no porosity is observed. Reports on obtaining GaAs have been published by the authors [20,21].

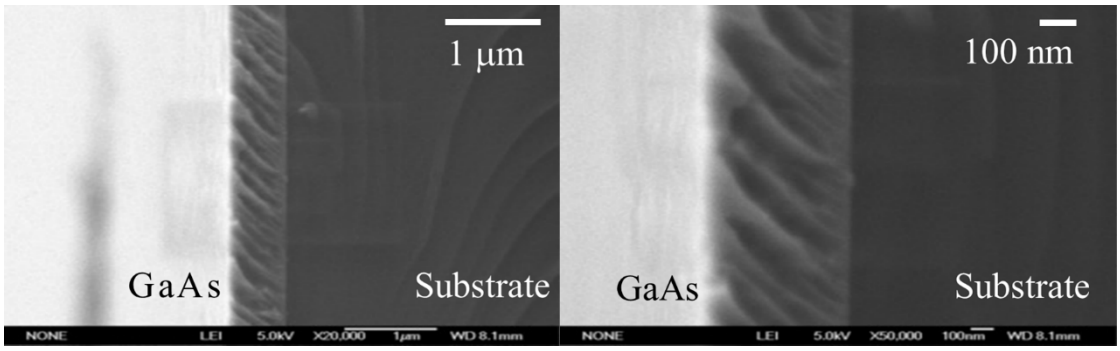

Fig. 2. Cross-sectional SEM images along of entire GaAs/Si layer thickness. Magnification-scale: 20.000X-1mμ (left) and 50.000X-100nm (right).

3.2. GaAs/Cr/GaAs layers

In Figure 3, the x-ray diffractograms of the bilayer (GaAs/Cr/GaAs) are presented with variations in the growth time (tg) of the intermediate Cr layer for 5 minutes (sample M1) and 10 minutes (sample M2). The growth temperature of the GaAs layer was maintained at 500 °C to prevent the segregation of Cr on the GaAs layer. In M1 (tg = 5 min), as observed in the spectra of Figure 3, distinct reflections from the (111), (102), (220), (004) planes are evident at 2θ = 27.49°, 41.9°, 39.5°, 46.9°, and 68.0°, respectively. These reflections correspond to the cubic GaAs crystalline structure with a lattice parameter of 0.5408 nm. Crystallographic planes such as (220) and (211) at 2θ = 81.2° and 85.6° are attributed to Cr from the interlayer [22]. Other planes at 39.3°, 62.90°, and 72° corresponding to CrGa and CrAs at 39.3° were also identified. These additional planes result from the diffusion of Cr on the Ga-As layer or GaAs on the Cr layer. The (200) plane located at 32.7° belongs to the Si substrate.

For the Cr interlayer growth for 10 minutes (labeled M2 in Figure 3), it is interesting to note that the X-ray spectrum of the M2 sample exhibits a better-defined structure than that of M1. This improvement in structure is attributed to the fact that the thickness (t) of the Cr interlayer in M2 is approximately two times larger than that in sample M1, considering a linear growth rate. In this case, the intensity of GaAs and Cr planes is roughly the same as in sample M1; however, the planes of the GaCr compound tend to disappear. Instead, new peaks at 52°, 64°, and 72° related to the CrAs compound emerge [23]. The formation of CrAs binary phases is particularly noteworthy due to their magnetic properties above room temperature, making them important for spintronic applications.

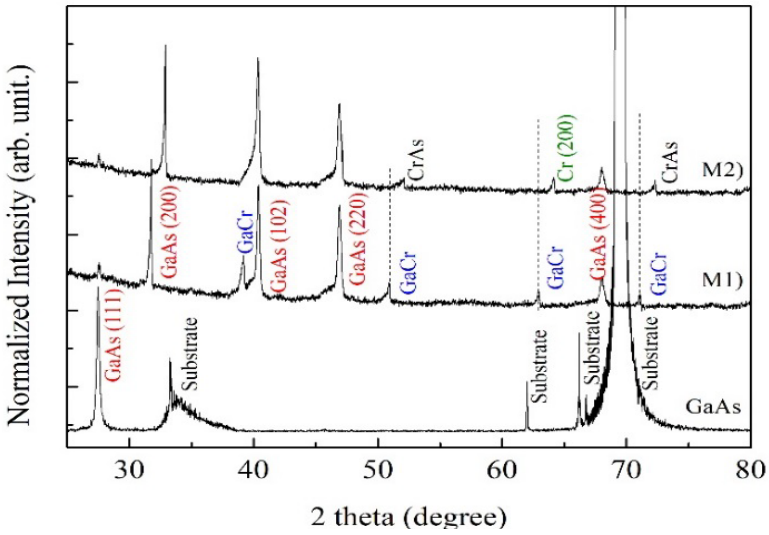

Fig. 3. X-ray spectra of GaAs/Cr/GaAs layers for time of growth Cr interlayer of 5 min (M1) and 10 min (M2).

Figure 4 presents the SEM image (100 nm scale, Mag = 134.07X) of the sample (M2) grown on a (100) Si substrate during a growth time of 10 minutes for the Cr interlayer. In this image, the well-defined thinnest layer of Cr (interlayer), approximately 70 nm thick, positioned between two layers of GaAs, is clearly distinguishable. The GaAs layer, oriented along the long (111) direction, exhibits a polycrystalline structure, and demonstrates a columnar growth mode in this image.

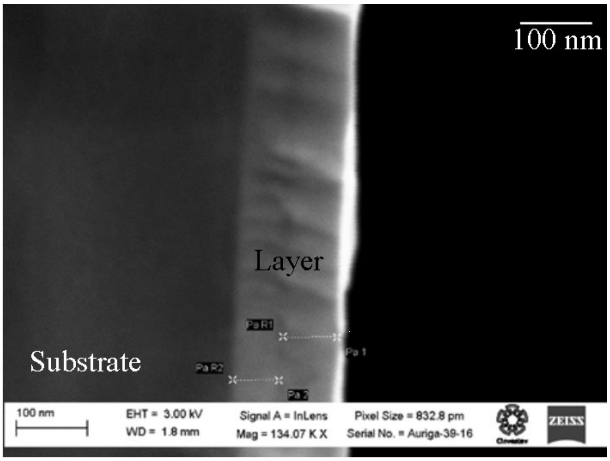

Fig. 4. Cross-section SEM image of the GaAs/Cr/GaAs layer for time growth of 10 min of the Cr interlayers. The image was taken in a 100nm scale and 134.07 KX magnification.

X-ray spectroscopy energy dispersive (EDS) measurements were conducted along the entire layer thickness to analyze the diffusion of Cr on the GaAs layer. In Fig. 5, an EDS line scan of the elements Ga (red line), As (green line), and Cr (blue line) within the GaAs/Cr/GaAs layers is presented.

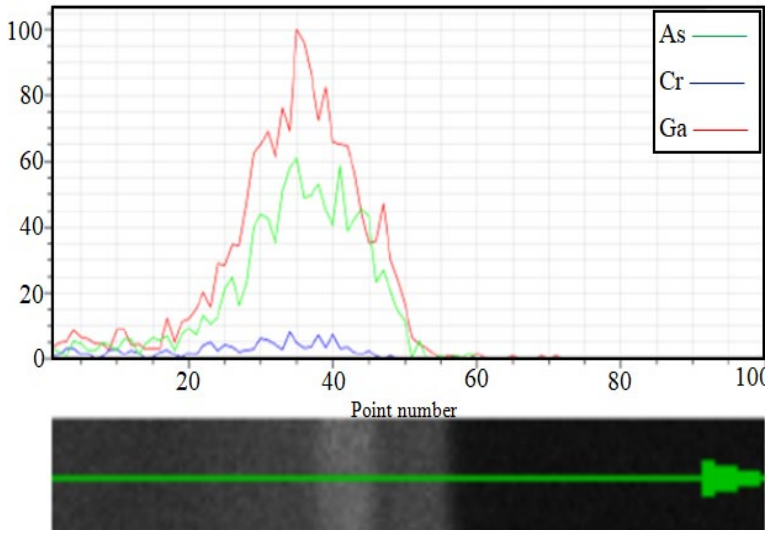

Fig. 5. EDS line scan performed along the entire GaAs/Cr/GaAs layers thickness. Line green (As), red line (Ga) and blue line (Cr) represent the elements present in the layers.

The elemental chemical analysis by EDS along the entire GaAs/Cr/GaAs layer thickness is summarized in Table 1. From this table, it is evident that the stoichiometric ratio of the GaAs binary compound has changed due to the inclusion of Cr. The EDS scans indicate that the GaAs layer now contains Cr, suggesting interfacial diffusion from the Cr layer to the GaAs layer, leading to the formation of CrAs and AsGa compounds [23], consistent with x-ray diffraction measurements (Fig. 3 M1-M2). While interdiffusion between Cr and GaAs has been reported in studies using epitaxy growth methods [24-26], the available results on Cr diffusion in GaAs prepared by r.f. magnetron sputtering are limited and scarce.

Table 1. Elemental Chemical Analysis by EDS. C [wt.%]: unnormalized concentration in weight percent of the element; norm. C [wt.%]: normalized concentration in weight percent of the element; C Atom. [at %]: atomic weight percent; C Error) [wt.%): the error in the weight percent concentration at the 1 sigma level.

E1	AN	Series	unn (wt%)	C. norm (wt%)	C. Atom (wt%)	C. Error (wt%)
Ga	31	L-series	5.97	41.78	39.44	0.64
As	33	L-series	4.85	33.95	29.82	1.63
Cr	24	L-series	3.47	24.27	30.74	0.59
		Total:	14.29	100	100	

Raman spectroscopy is a highly suitable technique for characterizing materials, especially doped semiconductor materials, owing to its high sensitivity in discriminating vibrational phonon modes from impurities or defects in the crystal structure of the host semiconductor. The Raman tensor is instrumental in predicting the relative intensity of the scattered radiation for different scattered geometries. According to Raman selection rules for the zinc blende (ZnS) crystal structure oriented along (111), the LO (Longitudinal Optical) and TO (Transverse Optical) modes are allowed. In this case, the intensity of the TO mode is greater than the LO mode [27].

In this study, to determine the phonon modes of the GaAs polycrystalline layer and the vibrating modes of GaCr and AsCr, Raman measurements were carried out using the 632 nm line of an Argon laser as an excitation source. The scattering beam was focused, producing a spot of 1 μm. The scattered light was recorded in backscattering geometry using a Dilor Labram Raman microscope equipped with an Olympus BX40.

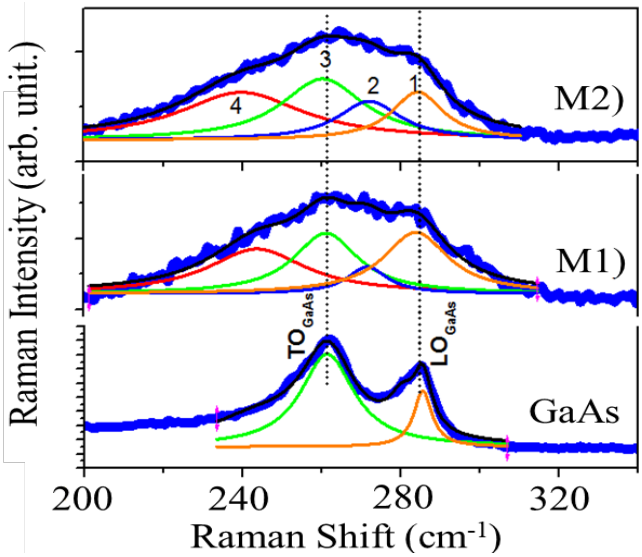

Fig. 5. Raman spectra of the GaAs layer taken as reference (M0). Raman spectra of the GaAs/Cr/GaAs layer grown on (001) Si, for the time of growth of 5 min (M1) and 10 min (M2) of the Cr interlayer. The color lines are the deconvolution of the Raman spectra into four Lorentzian functions corresponding to the vibrational phonon modes of GaAs amorphous (4), TO-GaAs (3), AsCr (2), and (1) LO-GaAs.

Figure 5 illustrates the first-order Raman spectra of a (M0) GaAs (111) layer and (M1)-(M2) Cr interlayers, deposited for 5 minutes and 10 minutes at room temperature, respectively. To analyze the Raman results, a deconvolution of the Raman spectra was performed using the Lorentzian function in the range from 200 to 350 cm^{-1}. For the (111) polycrystalline GaAs layer, the characteristic LO (Longitudinal Optical) and TO (Transverse Optical) vibrational modes at 261 cm^{-1} and 284 cm^{-1} were clearly observed.

The integrated intensity ratio (I_{TO}: I_{LO} = 5.34) obtained from the deconvolution of the Raman spectra using two Lorentzian functions (red and green lines) indicates that the (111) GaAs layer has good crystalline quality, consistent with Raman selection rules for the (111) plane. The TO and LO phonon modes of the (111) GaAs exhibit a redshift of 10 cm^{-1} compared to the reported value for GaAs/Si(100) possibly due to the lattice parameter mismatch (4%) with the Si (100) substrate [28].

After the growth of a Cr interlayer for 5 minutes (M2) and 10 minutes (M3), the Raman line shape in Fig. 5 (M2) - (M3) significantly differs from the (111) GaAs spectra, which is narrow and more symmetric. The Raman lines of the (M2) and (M3) layers are asymmetric and show an increase towards lower frequencies as the Cr interlayer growth time is extended from 5 minutes to 10 minutes. In these spectra, four peaks labeled as (1), (2), (3), and (4) corresponding to LO (Longitudinal Optical) (3) and TO (Transverse Optical) (1) phonon modes GaAs-like are identified. The integrated intensity (ITO/ILO) ratio remains approximately the same, and there is no observed shift (cm^{-1}) in the position of the LO and TO phonon modes GaAs-like.

A broader band centered around 240 cm^{-1} (4) corresponds to the amorphous mode of GaAs [29]. This gives rise to the Disorder-Activated Acoustic Mode (DALA) (100 cm^{-1} < k < 200 cm^{-1}), which is a longitudinal acoustic mode activated by electronic states due to the disorder in the crystal field [30, 31]. Deformation of the line shape in the Raman spectrum between LO and TO vibrational phonon modes of GaAs is possible due to the substitution of As by Cr through inter-diffusion at the interface, generating local vibration modes (LVM) of CrAs (mode 2). The incorporation of Cr in GaAs results in a symmetry breaking of the lattice from a harmonic potential due to local lattice disruption [32]. An LVM (local vibration mode) requires a high impurity concentration to be observed, and its influence on the optical phonon modes is very noticeable.

3. Conclusions

In this article, we have presented the results of the growth and characterization of a GaAs layer and GaAs/Cr/GaAs polycrystalline layers. EDX spectra revealed that chromium diffused from the Cr interlayer towards the GaAs layer, reacting with As and Ga to form CrAs and CrGa compounds. The inclusion of Cr induced structural disorder in the GaAs host. Notably, the appearance of a phonon mode of CrAs between the TO and LO GaAs modes contributed to the deformation of the Raman line shape from 260 to 285 cm^{-1}.

The use of magnetron sputtering, which involves the deposition of alternating layers of GaAs and Cr, emerges as a promising approach to obtaining semiconductors with satisfactory structural and morphological properties for potential optoelectronic applications. Exploring semiconductor alloys, such as GaAs, combined with transition metals like Cr, opens up possibilities for applications in various fields of current and future technology.

Acknowledgments

The authors thank the technical assistance of Ms-Ing. Alvaro Angeles Pascual, Laboratorio Avanzado de Nanoscopia del Centro de Investigación y de Estudios Avanzados del I.P.N. Special thanks to Laboratorio de Materiales Nanoestructurados y Funcionales de la Universidad Nacional de Colombia, sede Manizales. This work was partially supported by Dirección de Investigaciones de Manizales (DIMA), Proyecto 38416.

References

[1] R. Chhavi Sharma, R. Nandal, N. Tanwar, R. Yadav, J. Bhardwaj, A. Verma, Journal of Physics: Conference Series, 2426, 012008 (2023); https://doi.org/10.1088/1742-6596/2426/1/012008
[2] S. Mokkapati, C. Jagadish, Materialstoday 12(4), 22 (2009); https://doi.org/10.1016/S1369-7021(09)70110-5
[3] J. K. Furdyna, X. Liu, M. Dobrowolska, S. Lee, Journal of Applied. Physics, 134, 200901 (2023); https://doi.org/10.1063/5.0176698
[4] A. V. Kudrin, V. P. Lesnikov, R. N. Kriukov, Y. A. Danilov, M. V. Dorokhin, A. A. Yakovleva, N. Yu. Tabachkova, N.A. Sobolev, Nanomaterials, 13(17), 2435 (2023); https://doi.org/10.3390/nano13172435
[5] M. Brozel, Springer Handbook of Electronic and Photonic Materials, 499–536, (2006); https://doi.org/10.1007/978-0-387-29185-7_23
[6] Y. Hee Lee, , Science, 382 (6668), (2023); https://doi.org/10.1126/science.adl0823
[7] T. Dietl, Nature Materials, 9, 965–974 (2010); https://doi.org/10.1038/nmat2898
[8] M. A. Green, E. D. Dunlop, M. Yoshita, N. Kopidakis, K. Bothe, G. Siefer, X. Hao, Progress in Photovoltaics: Research and Applications, 32(1), 3-13 (2023); https://doi.org/10.1002/pip.3750
[9] H. Morkoç A. Y. Cho, Journal of Applied Physics 50, 6413 (1979); https://doi.org/10.1063/1.325732
[10] B. D. Milbrath, A. J. Peurrung, M. Bliss, J. Weber, Journal of Materials Research, 23(10), 2561 (2008); https://doi.org/10.1557/JMR.2008.031
[11] M. B. Haider, R. Yang, H. Al-Brithen, C. Constantin, D. C. Ingram, A. R. Smith, G. Caruntu, C. J. O'Connor, Journal of Crystal Growth, 285(3), 300 (2005); https://doi.org/10.1016/j.jcrysgro.2005.08.047
[12] S. Ilahi, Physica B: Condensed Matter, 652(1), 414612 (2023); https://doi.org/10.1016/j.physb.2022.414612
[13] J. Xue, W. Chen, T. Tao, T. Zhi, P. Shao, Q. Cai, G. Yang, J. Wang, D. Chen, R. Zhang, Journal of Applied. Physics, 134, 143904 (2023); https://doi.org/10.1063/5.0165709

[14] M. Mizuguchi, H. Akinaga, T. Manago, K. Ono, M. Oshima, M. Shirai, M. Yuri, H. J. Lin, H. H. Hsieh, and C. T. Chen, Journal of Applied Physics 91, 7917 (2002); https://doi.org/10.1063/1.1455612
[15] D. Qian, G.L. Liu, D. Loison, G.S. Dong, X.F. Jin, Journal of Crystal Growth 218(2-4), 197 (2000); https://doi.org/10.1016/S0022-0248(00)00545-5
[16] J. L. Xu, M van Schilfgaarde, G D Samolyuk, Physical Review Letters, **94(9-11),** 097201 (2005); https://doi.org/10.1103/PhysRevLett.94.097201
[17] H. J. Stocker, M.Schmidt, Journal of Applied Physics 47, 2450 (1976); https://doi.org/10.1063/1.322956
[18] A. Pulzara-Mora, C. Pulzara-Mora, A. Forero-Pico, M. Ayerbe-Samaca, J. Marqués-Marchán, A. Asenjo, N.M. Nemes, D. Arenas, R. Sáez Puche" Thin Solid Films, 705 137971, (2020); https://doi.org/10.1016/j.tsf.2020.137971
[19] Á. Pulzara Mora, J. G. Doria Andrade, C. A. Pulzara Mora, R. Bernal Correa, A. Rosales Rivera, Materia (Rio J), 25(2), 12784 (2020); https://doi.org/10.1590/S1517-707620200004.1184
[20] R. Bernal Correa, J. Montes Monsalve, A Pulzara Mora, M. López López, A. Cruz Orea, J. A. Cardona, Superficies Vacio, 27(3), 102 (2014).
[21] R. Bernal-Correa, S. Gallardo-Hernández, J. Cardona-Bedoya, A. Pulzara-Mora, Optik, 14, 608 (2017) https://doi.org/10.1016/j.ijleo.2017.08.042
[22] S. L. Duan and J. O. Artman, B. Wong and D.E. Laughlin. J. Applied Physics, 67 (9), 4913 (1990); http://dx.doi.org/10.1063/1.344729
[23] T. S. Huang, M. S. Yang, Journal of Applied Physics 70, 5675 (1991); http://dx.doi.org/10.1063/1.350184
[24] J. H. Weaver, M. Grioni, J. Joyce, Physical Review B, 31(8), 5348 (1985); http://dx.doi.org/10.1103/PhysRevB.31.5348
[25] H. Akinaga, T. Manago, M. Sirai, Japanese Journal of Applied Physics, 39, L1118 (2000); http://dx.doi.org/10.1143/JJAP.39.L1118
[26] D. H. Mosca, P. C. de Camargo, J. L. Guimaraes, W. H. Schreiner, A. J. A. de Oliveira, P. E. N. Souza, M. Eddrief, V. H. Etgens. Journal of Physics: Condensed Matter, 17(43), 6805 (2005); http://dx.doi.org/10.1088/0953-8984/17/43/002
[27] P. Yu, M. Cardona, Fundamentals of Semiconductors. Berlin Heidelberg New York: Springer, 2005.
[28] B. Roughani, M. Kallergi, J. Aubel S. Sundaram, Journal of Applied Physics, 66 4946 (1989); http://dx.doi.org/10.1063/1.343766
[29] G. Burns, F. H. Dacol, C. R. Wie, E. Bursteint M. Cardona, Solid State Communications, 62(7) 449 (1987); http://dx.doi.org/10.1016/0038-1098(87)91096-9
[30] M. Holtz and R. Zallen, O. Brafman, Physical Review Volume 38(9), 6097 (1997); http://dx.doi.org/10.1103/PhysRevB.38.6097
[31] H. Kawamura, R. Tsu, L. Esaki, Physical Review Letters 29 (20), 1397 (1972); https://doi.org/10.1103/PhysRevLett.29.1397
[32] K. Sen, Y. Yao, R. Heid, A. Omoumi, F. Hardy, K. Willa, M. Merz, A. A. Haghighirad, M. Le Tacon. Physical Review B, 100(10), 104301 (2019); https://doi.org/10.1103/PhysRevB.100.104301